Modeling Groundwater Flow in Unconfined Conditions of Variable Density Solutions in Dual-Porosity Media Using the GeRa Code

Ivan Kapyrin✉[1,2], Igor Konshin[2,3], Vasily Kramarenko[2], and Fedor Grigoriev[1,2]

[1] Nuclear Safety Institute of the Russian Academy of Sciences (IBRAE), Moscow 115191, Russia
[2] Marchuk Institute of Numerical Mathematics of the Russian Academy of Sciences (INM RAS), Moscow 119333, Russia
[3] Dorodnicyn Computing Centre (FRC CSC RAS), Moscow 119333, Russia

ivan.kapyrin@gmail.com, igor.konshin@gmail.com, kramarenko.vasiliy@gmail.com, grig-fedor@yandex.ru

Abstract. Flow of variable density solution in unconfined conditions and transport in dual-porosity media mathematical model is introduced. We show the application of the model to a real object which is a polygon of deep well liquid radioactive waste injection. Several assumptions are justified to simplify the model and it is discretized. The model is aimed at assessment of the role of density changes on the contaminant propagation dynamics within the polygon. The method of parallelization is described and the results of numerical experiments are presented herein.

Keywords: Parallel Computing · Density-Driven Flow · Dual-Porosity Media · Unconfined Flow · Liquid Waste Deep Injection

1 Introduction

Simulation of groundwater (GW) flow in unconfined regime with allowance for density convection and the effect of double porosity is quite an exotic task, poorly studied in the scientific literature. The necessity to develop this model was stipulated by the practical task of assessing the effect of the density driven convection effect on the dynamics of the spreading of contaminants on the polygon of liquid radioactive waste (LRW) deep disposal "Severny" [1, 2]. The "Severny" polygon is located in the Krasnoyarsk Territory. In the deep (more than 400 m) I-st horizon, since 1967, injection of solutions with a high mineralization (up to 200 g/l) has been carried out. In the geoflow-geomigration model of the "Severny" polygon, GEOPOLIS, developed by the Nuclear Safety Institute of the RAS, the process of density driven convection was not taken into account, and in the process of improving this model, the question arose about the need to simulate it.

The transition from the conventional flow and transport model to the model, taking into account the density driven convection, is associated with a significant

increase in the complexity of the model and slowing down the calculations, as the processes of flow and transport in porous media become strongly coupled thus no longer allowing to divide the solution of the problem into two (flow and transfer) at each time step. Note that the rate of computations is quite critical for the polygon model, since when calibrating the model parameters calculations have to be performed repeatedly. In addition, to ensure the necessary accuracy of calculations and the stability of the calculation schemes (using the explicit low-dissipation scheme of discretization of the advection operator), the time step for this model should not exceed 10 days for a total simulation period of 50 years for epigenetic calculations. Thus, it is necessary to determine how essential the process of density driven convection is for the rate of migration of radionuclides in the underground aquifers of the polygon. Based on the final results of this study, the process of density driven convection must either be included in the model, or be reasonably ignored in the simulation, which will save the computational time.

In the present paper, a mathematical model is derived, simplifying assumptions are justified, and parallel calculations are performed to demonstrate the applicability and efficiency of the model. The model is implemented in the GeRa (**Ge**omigration of **Ra**dionuclides) computational code developed by IBRAE and INM RAS for solving the problems of radioactive waste disposal safety assessment [3, 4] on unstructured 3D grids [5]. Parallelization is done using MPI, which is a common trend for similar contemporary hydrogeological codes, such as PFLOTRAN [6], Amanzi [7] and TOUGH2-MP [8].

2 Mathematical Model

Let us formulate the complete system of equations of the GW flow model under conditions of variable saturation and transport taking into account double porosity and density driven convection:

$$\begin{cases} \frac{\partial(S_{\mathrm{m}}\varphi_{\mathrm{m}}\rho_{\mathrm{m}})}{\partial t} + \nabla\cdot(\rho_{\mathrm{m}}\boldsymbol{u}) = Q\rho_s - \rho_{\mathrm{exch}}\Gamma_w, \\ \frac{\partial\theta_{\mathrm{im}}}{\partial t} = \Gamma_w, \\ \frac{\partial\left(\left(\theta_{\mathrm{m}}+\rho_{b_{\mathrm{m}}}k_{d_{i,\mathrm{m}}}\right)C_{i,\mathrm{m}}\right)}{\partial t} + \lambda\left(\theta_{\mathrm{m}}+\rho_{b_{\mathrm{m}}}k_{d_{i,\mathrm{m}}}\right)C_{i,\mathrm{m}} + \nabla\left(\boldsymbol{u}C_{i,\mathrm{m}}\right) \\ \qquad - \nabla D_{i,\mathrm{m}}\nabla C_{i,\mathrm{m}} + \zeta\left(C_{i,\mathrm{m}} - C_{i,\mathrm{im}}\right) = QC_{i,s} - C_{\mathrm{exch}}\Gamma_w, \\ \frac{\partial\left(\left(\theta_{\mathrm{im}}+\rho_{b_{\mathrm{im}}}k_{d_{i,\mathrm{im}}}\right)C_{i,\mathrm{im}}\right)}{\partial t} + \lambda\left(\theta_{\mathrm{im}}+\rho_{b_{\mathrm{im}}}k_{d_{i,\mathrm{im}}}\right)C_{i,\mathrm{im}} \\ \qquad = \zeta\left(C_{i,\mathrm{m}} - C_{i,\mathrm{im}}\right) + C_{\mathrm{exch}}\Gamma_w, \qquad i = 1,\ldots,N_{\mathrm{comp}}. \end{cases} \tag{1}$$

In system (1), the third and fourth equations are written out for each of the components carried in the solution, the index i denotes the component number, N_{comp} is the total number of components. The subscripts "m" and "im" mean that the variable or coefficient belongs to the mobile and immobile zones, respectively. Here the following notations are used (in square brackets the dimension of the quantity is indicated: M, L, and T stand for mass, length, and

time, respectively, while [-] means dimensionless value): S is saturation, [-]; θ is the moisture content, [-] associated with the saturation by the formula:

$$S = \frac{\theta}{\varphi}; \tag{2}$$

where φ is the porosity of the medium, [-], composed of the porosity of the flow zone; φ_{m} and φ_{im} are the mobile and immobile zone porosities; ρ is the density of the solution, [ML^{-3}]; $\boldsymbol{u}$ is the Darcy velocity vector, [LT^{-1}]; ρ_s is the density of the solution in sources or sinks, [ML^{-3}]. Q is the volumetric flow rate of the fluid sources or sinks (usually wells), [T^{-1}]; Γ_w is the intensity of moisture exchange between the mobile and immobile zones, [T^{-1}]; ρ_{exch} and C_{exch} is the density of the liquid and the concentration of the impurity in the solution flowing from the mobile to the immobile zone:

$$\rho_{\mathrm{exch}} = \begin{cases} \rho_{\mathrm{m}}, & \Gamma_w \geq 0, \\ \rho_{\mathrm{im}}, & \Gamma_w < 0; \end{cases} \qquad C_{\mathrm{exch}} = \begin{cases} C_{\mathrm{m}}, & \Gamma_w \geq 0, \\ C_{\mathrm{im}}, & \Gamma_w < 0; \end{cases}$$

ρ_b is the rock density, [ML^{-3}]; k_d is the distribution coefficient, [$\mathrm{M}^{-1}\mathrm{L}^3$]; C is the contaminant concentration, [ML^{-3}]; D is the diffusion-dispersion tensor, [$\mathrm{L}^2\mathrm{T}^{-1}$]; ζ is the mass exchange coefficient between the mobile and immobile zones, [T^{-1}].

Note that in this case the first order rate dual-porosity model [9] is used. The system of equations (1) must be supplemented by a number of constitutive relations. First, it is the generalized Darcy's law for the dependence of Darcy velocity on the equivalent freshwater head h, [L] and density:

$$\boldsymbol{u} = -K\left(\nabla h_{\mathrm{m}} + \frac{\rho - \rho_0}{\rho_0}\nabla z\right), \tag{3}$$

where K is the hydraulic conductivity, [LT^{-1}]; ρ_0 is the reference density of the liquid in the absence of contaminants, [ML^{-3}]; z is the vertical coordinate, [L].

Note that here the equivalent freshwater head (later on simply called head) is used, expressed in meters of the water column of the reference liquid (a solution with a reference density ρ_0, without impurities). In fact, if p is pressure, then

$$h = \frac{p}{\rho_0 g} + z,$$

where g is the gravity constant, [LT^{-2}].

Secondly, the density of the liquid depends on the concentration. Let's put it linear:

$$\rho = \rho_0 + \sum_{i=1}^{N_{\mathrm{comp}}} \varkappa_{\mathrm{vol},i} C_i. \tag{4}$$

Here $\varkappa_{\mathrm{vol},i}$ is the volumetric expansion coefficient, [-]. The linear dependence of this type is quite justified not only for small impurity concentrations, but in some cases also for high concentrations. Specifically for the "Severny" polygon, the main component determining the density of the solution is sodium nitrate,

and according to [10], a linear dependence of the form (4) with a coefficient of volumetric expansion of approximately 0.6 can be used.

Third, the intensity Γ_w of the flow between the mobile and immobile zones should be determined. These formulas may be found, for example, in [11], but we omit them here as they will be excluded from the model later on.

When solving the problem (1), the change in porosity is usually neglected, considering it to be constant, and taking into account only the time derivative of the porosity. Then, similarly to [12–14] for the time derivative in the first equation of system (1) we will use the representation:

$$\frac{\partial \left(S_{\mathrm{m}} \varphi_{\mathrm{m}} \rho_{\mathrm{m}}\right)}{\partial t} \approx \rho_{\mathrm{m}} \frac{\partial \theta_{\mathrm{m}}}{\partial t} + S_{\mathrm{m}} \rho_{\mathrm{m}} s_{\mathrm{stor}} \frac{\partial h}{\partial t} + \theta_{\mathrm{m}} \sum_{i=1}^{N_{\mathrm{comp}}} \varkappa_{\mathrm{vol},i} \frac{\partial C_i}{\partial t}. \tag{5}$$

Due to the complexity of both the mathematical model (1) and its practical parameterization, let's consider the possible simplifications of system (1) that are relevant for the "Severny" polygon model. An essential feature of this problem has to be focused on: LRW propagation occurs in deep aquifers in a saturated pressure regime. This means that the effect of dual porosity is not significant for the upper layers of the model (1–2 layers) in the zone of variable saturation, since, firstly, pollution does not reach them, and secondly, the moisture exchange between the mobile and immobile zones can be neglected, supposing that the model of flow in a single porousity medium is sufficient to describe the flow process in this region. In turn, for the reservoirs of RAW, flow processes in a medium with variable saturation are not relevant. This factor taken into account in the model it can be assumed that the change in saturation refers only to the mobile zone, and the saturation of the immobile zone does not change.

Indeed, in the fully saturated zone of the GEOPOLIS model, the saturation does not change either in the mobile or in the immobile zones. Besides, in the zone of partial saturation, the presence of an immobile zone with constant saturation reduces the flow problem to the standard flow problem in a single porousity medium, while the effect of the presence of the immobile zone on transport remains. But the transport for the GEOPOLIS model, first, is not significant in the unsaturated zone (pollution does not reach it), and second, this model in any case provides wider possibilities for calculating the transfer in the unsaturated region due to the presence of a mass exchange coefficient ζ. The latter, like other coefficients, can be calibrated. In the upper layers, where it is possible to form a zone of variable saturation, the model reduces to transport in a single porosity vadose zone. Thus, we can take

$$\theta_{\mathrm{im}} = \varphi_{\mathrm{im}}, \qquad \Gamma_w = 0. \tag{6}$$

Given the assumptions made (5)–(6), the model (1) is converted to the form:

$$\begin{cases} \rho_{\mathrm{m}} \frac{\partial \theta_{\mathrm{m}}}{\partial t} + S_{\mathrm{m}} \rho_{\mathrm{m}} s_{\mathrm{stor}} \frac{\partial h}{\partial t} + \theta_{\mathrm{m}} \sum\limits_{i=1}^{N_{\mathrm{comp}}} \varkappa_{\mathrm{vol},i} \frac{\partial C_i}{\partial t} + \nabla \cdot (\rho_{\mathrm{m}} \boldsymbol{u}) = Q \rho_s, \\ \frac{\partial \left(\left(\theta_{\mathrm{m}} + \rho_{b_{\mathrm{m}}} k_{d_{i,\mathrm{m}}} \right) C_{i,\mathrm{m}} \right)}{\partial t} + \lambda \left(\theta_{\mathrm{m}} + \rho_{b_{\mathrm{m}}} k_{d_{i,\mathrm{m}}} \right) C_{i,\mathrm{m}} + \nabla \left(\boldsymbol{u} C_{i,\mathrm{m}} \right) \\ \qquad - \nabla D_{i,\mathrm{m}} \nabla C_{i,\mathrm{m}} + \zeta \left(C_{i,\mathrm{m}} - C_{i,\mathrm{im}} \right) = Q C_{i,s}, \\ \varphi_{\mathrm{im}} R_{\mathrm{im}} \frac{\partial C_{i,\mathrm{im}}}{\partial t} + \lambda \varphi_{\mathrm{im}} R_{\mathrm{im}} C_{i,\mathrm{im}} = \zeta \left(C_{i,\mathrm{m}} - C_{i,\mathrm{im}} \right), \quad i = 1, \ldots, N_{\mathrm{comp}}. \end{cases} \tag{7}$$

In (7), the retardation factor in the immobile zone was introduced, [-]:

$$R_{i,\mathrm{im}} = \left(1 + \frac{\rho_b}{\varphi_{\mathrm{im}}} k_{d_{i,\mathrm{im}}} \right). \tag{8}$$

The index "m" in the flow equation will be omitted here, since in this model there are no corresponding variables for the immobile zone. It is necessary to supply the system with dependences $\theta(h), K(h)$. To simulate the flow in unconfined regime, we will use a pseudo-saturated formulation, a similar approach is proposed in [12]. It is more convenient to write out the dependence for the moisture content in terms of the pressure head, and then use formula for the transition from ψ to h:

$$h = \psi + z. \tag{9}$$

It is assumed that $\theta(\psi)$ has two intervals of linear dependence on the pressure head ψ:

$$\theta(\psi) = \begin{cases} \varphi, & \psi > 0, \\ \varphi - \frac{\varphi(1-\alpha_\phi)}{\psi_r}, & \psi_r < \psi < 0, \\ \varphi \left(\alpha_\phi - \alpha_\theta \left(\psi_r - \psi \right) \right), & \psi_r > \psi. \end{cases} \tag{10}$$

There are three parameters in the model: $(\alpha_\phi, \alpha_\theta, \psi_r)$. The first two are dimensionless, the latter has dimension [L]. The principles of choosing these parameters should be described. Note that $\theta(\psi_r) = \alpha_\varphi \varphi$ is a quantity that is an analog of the residual moisture content in unsaturated flow models. The parameter α_θ characterizes the slope of $\theta(\psi)$ as ψ decreases below ψ_r. The parameter ψ_r characterizes the value of the pressure head at which the rock is close to dry. We follow the basic principle of flow modeling in unconfined conditions: the presence of a sharp boundary between fully saturated and dry media, and the possibility of fluid flow only in saturated region. In this case, the parameters α_θ and α_ϕ should be chosen sufficiently small ($\ll 1$), and the parameter ψ_r should be equal to the characteristic vertical dimension of the grid cell, when the groundwater level in the cell fell by a given amount, it could be considered drained, containing only residual moisture. We also note that when choosing the parameter α_θ, it is necessary to ensure the nonnegativity of $\theta(\psi)$, that is, with the maximum possible drop in the pressure head, the moisture content should be at least zero. In the case of the "Severny" polygon model, the following parameters were selected, thus providing the above properties of the model:

$$\alpha_\phi = 0.1, \quad \alpha_\theta = 0.001, \quad \psi_r = -30 \text{ m}. \tag{11}$$

For the $K(h)$ dependence, the following expression is accepted:

$$K(h) = K_r(h)K_s, \tag{12}$$

where K_s is the saturated hydraulic conductivity and the relative permeability $K_r(h)$ is identically equal to the saturation of $S(h)$:

$$K_r(h) = S(h). \tag{13}$$

Thus, the improved mathematical model of flow and transport at the "Severny" polygon which allows for the unconfined regime of the flow and the presence of weakly permeable interlayers in aquifers (dual porosity), consists of a system of equations (7), the constitutive equations (3), (4), (10), (13), the relation (9) between the variables h and ψ.

3 Discretization of the Model in Time and Space

For the diffusion operator, including the flow problem, the finite volume method (FV) is used with a linear two-point flow approximation scheme. To discretize the convection operator we use the FV explicit TVD-scheme with piecewise linear reconstruction of the concentration on the computational grid cells. Since the calculations of the model take very long time, and the use of the explicit scheme imposes a significant limitation on the time step (about 1 day), a transition to the use of an implicit FVM scheme of the first order of accuracy for approximation of the convective term is possible. The latter will allow one to remove restrictions on the time step and significantly accelerate the calculations especially when carrying out long-term forecasts. To discretize the last equation in (7) we will use an implicit scheme. In general, to solve the transport problem (the second and third equations (7)) we use splitting by physical processes. This will make it possible to separate the solution of the mass exchange problem from the transport and flow problems. To discretize the solution of the coupled flow-transport problem (7) we use the sequential iterative scheme. We represent the discrete system of equations corresponding to the system of differential equations (7) in the following form:

$$\begin{cases} F\left(h^{n+1}, C_{\mathrm{m}}^{n+1}\right) = 0, \\ T\left(h^{n+1}, C_{\mathrm{m}}^{n+1}, C_{\mathrm{im}}^{n+1}\right) = 0, \\ E\left(C_{\mathrm{m}}^{n+1}, C_{\mathrm{im}}^{n+1}\right) = 0. \end{cases} \tag{14}$$

Here $h^{n+1}, C_{\mathrm{m}}^{n+1}, C_{\mathrm{im}}^{n+1}$ are the vectors of equivalent freshwater heads and concentrations in the mobile and immobile zones in cells of the computational grid at the next, $(n+1)$-th time step. The system (14) consists of three subsystems of nonlinear equations. The first one, $F\left(h^{n+1}C_{\mathrm{m}}^{n+1}\right) = 0$, corresponds to the flow equation, that is, to the first equation in (7). The second, $T\left(h^{n+1}, C_{\mathrm{m}}^{n+1}, C_{\mathrm{im}}^{n+1}\right) = 0$, consists of discrete transport equations corresponding to the second equation of (7). The third subsystem corresponds to the last equation of the system (7)

and describes the mass transfer between the mobile and immobile zones. To solve the nonlinear system (14), the fixed point iteration method is used. In this case, the time step of the scheme is constructed as follows:

1. As the initial guess, the values from the previous time step are selected: $h^{n+1,0} = h^n$, $C_{\mathrm{m}}^{n+1,0} = C_{\mathrm{m}}^n$. The iteration counter $k = 0$ is set.
2. The flow problem with density and concentration from the previous iteration is calculated: $F\left(h^{n+1,k+1}, C_{\mathrm{m}}^{n+1,k}\right) = 0$. The head $h^{n+1,k+1}$ and the corresponding flow $\boldsymbol{u}^{n+1,k+1}$, the moisture content $\theta_{\mathrm{m}}^{n+1,k+1}$ are calculated.
3. The transport problem with a known flux $\boldsymbol{u}^{n+1,k+1}$ is calculated:

$$\begin{cases} T\left(h^{n+1,k+1}, C_{\mathrm{m}}^{n+1,k+1}, C_{\mathrm{im}}^{n+1,k+1}\right) = 0, \\ E\left(C_{\mathrm{m}}^{n+1,k+1}, C_{\mathrm{im}}^{n+1,k+1}\right) = 0. \end{cases} \tag{15}$$

   From here there are concentrations on the new iteration $C_{\mathrm{m}}^{n+1,k+1}$, $C_{\mathrm{im}}^{n+1,k+1}$.
4. The iteration count is updated: $k = k + 1$.
5. The criterion for the convergence of the iterative process is checked. If the criterion is satisfied, we set $h^{n+1} = h^{n+1,k}$, $C_{\mathrm{m}}^{n+1} = C_{\mathrm{m}}^{n+1,k}$, $C_{\mathrm{im}}^{n+1} = C_{\mathrm{im}}^{n+1,k}$. Otherwise, go back to step 2.

The solution of the transport problem (15) has to be explained. The system of transport equations which is solved at each time step, has the form:

$$\begin{cases} \frac{\left(\theta_{\mathrm{m}}^{n+1,k+1} + \rho_b k_{d_{i,\mathrm{m}}}\right) C_{i,\mathrm{m}}^{n+1,k+1} - \left(\theta_{\mathrm{m}}^{n} + \rho_b k_{d_{i,\mathrm{m}}}\right) C_{i,\mathrm{m}}^{n}}{\triangle t} + \lambda \left(\theta_{\mathrm{m}}^{n+1,k+1} + \rho_b k_{d_{i,\mathrm{m}}}\right) C_{i,\mathrm{m}}^{n+1,k+1} \\ \qquad + \nabla \left(\boldsymbol{u}^{n+1,k+1} C_{i,\mathrm{m}}^{n}\right) - \nabla D_{i,\mathrm{m}} \nabla C_{i,\mathrm{m}}^{n+1,k+1} \\ \qquad + \zeta \left(C_{i,\mathrm{m}}^{n+1,k+1} - C_{i,\mathrm{im}}^{n+1,k+1}\right) = Q C_{i,z}^{n+1,k+1}, \\ \varphi_{\mathrm{im}} R_{\mathrm{im}} \frac{C_{i,\mathrm{im}}^{n+1,k+1} - C_{i,\mathrm{im}}^{n}}{\triangle t} + \lambda \varphi_{\mathrm{im}} R_{\mathrm{im}} C_{i,\mathrm{im}}^{n+1,k+1} = \zeta \left(C_{i,\mathrm{m}}^{n+1,k+1} - C_{i,\mathrm{im}}^{n+1,k+1}\right), \\ \qquad i = 1, \ldots, N_{\mathrm{comp}}. \end{cases} \tag{16}$$

Here we use the explicit approximation in time of the convection operator originally used in GEOPOLIS, and the implicit ones for all other operators. The possibility of an implicit approximation of convection will be explained later. We introduce the intermediate values of the concentration in the mobile zone $\hat{C}_{i,\mathrm{m}}^{n+1,k+1}, \tilde{C}_{i,\mathrm{m}}^{n+1,k+1}$ in order to use the splitting according to the physical processes to solve equation (16). We rewrite the time derivative of the first

equation of (16) using the intermediate concentration values:

$$\begin{aligned}
&\frac{\left(\theta_{\mathrm{m}}^{n+1,k+1}+\rho_b k_{d_{i,\mathrm{m}}}\right) C_{i,\mathrm{m}}^{n+1,k+1}-\left(\theta_{\mathrm{m}}^{n}+\rho_b k_{d_{i,\mathrm{m}}}\right) C_{i,\mathrm{m}}^{n}}{\triangle t} \\
&\quad=\frac{\left(\theta_{\mathrm{m}}^{n+1,k+1}+\rho_b k_{d_{i,\mathrm{m}}}\right)\left(C_{i,\mathrm{m}}^{n+1,k+1}-\hat{C}_{i,\mathrm{m}}^{n+1,k+1}+\hat{C}_{i,\mathrm{m}}^{n+1,k+1}-\tilde{C}_{i,\mathrm{m}}^{n+1,k+1}+\tilde{C}_{i,\mathrm{m}}^{n+1,k+1}\right)}{\triangle t} \\
&\qquad-\frac{\left(\theta_{\mathrm{m}}^{n}+\rho_b k_{d_{i,\mathrm{m}}}\right) C_{i,\mathrm{m}}^{n}}{\triangle t} \\
&\quad=\left(\theta_{\mathrm{m}}^{n+1,k+1}+\rho_b k_{d_{i,\mathrm{m}}}\right)\frac{C_{i,\mathrm{m}}^{n+1,k+1}-\tilde{C}_{i,\mathrm{m}}^{n+1,k+1}}{\triangle t}+\left(\theta_{\mathrm{m}}^{n+1,k+1}+\rho_b k_{d_{i,\mathrm{m}}}\right) \\
&\qquad\times\frac{\tilde{C}_{i,\mathrm{m}}^{n+1,k+1}-\hat{C}_{i,\mathrm{m}}^{n+1,k+1}}{\triangle t}+\frac{\left(\theta_{\mathrm{m}}^{n+1,k+1}+\rho_b k_{d_{i,\mathrm{m}}}\right)\hat{C}_{i,\mathrm{m}}^{n+1,k+1}-\left(\theta_{\mathrm{m}}^{n}+\rho_b k_{d_{i,\mathrm{m}}}\right) C_{i,\mathrm{m}}^{n}}{\triangle t}.
\end{aligned} \tag{17}$$

Then the splitting scheme is to be written as follows (step-by-step, for each component $i=1,\ldots,N_{\mathrm{comp}}$):

I:

$$\frac{\left(\theta_{\mathrm{m}}^{n+1,k+1}+\rho_b k_{d_{i,\mathrm{m}}}\right)\hat{C}_{i,\mathrm{m}}^{n+1,k+1}-\left(\theta_{\mathrm{m}}^{n}+\rho_b k_{d_{i,\mathrm{m}}}\right) C_{i,\mathrm{m}}^{n}}{\triangle t}+\nabla\left(\boldsymbol{u}^{n+1,k+1} C_{i,\mathrm{m}}^{n}\right)=Q C_{i,z}^{n+1},$$

II:

$$\begin{aligned}
&\left(\theta_{\mathrm{m}}^{n+1,k+1}+\rho_b k_{d_{i,\mathrm{m}}}\right)\frac{\tilde{C}_{i,\mathrm{m}}^{n+1,k+1}-\hat{C}_{i,\mathrm{m}}^{n+1,k+1}}{\triangle t}+\lambda\left(\theta_{\mathrm{m}}^{n+1,k+1}+\rho_b k_{d_{i,\mathrm{m}}}\right)\tilde{C}_{i,\mathrm{m}}^{n+1,k+1} \\
&\qquad-\nabla D_{i,\mathrm{m}}\nabla C_{i,\mathrm{m}}^{n+1,k+1}=0,
\end{aligned} \tag{18}$$

III:

$$\begin{cases}
\left(\theta_{\mathrm{m}}^{n+1,k+1}+\rho_b k_{d_{i,\mathrm{m}}}\right)\frac{C_{i,\mathrm{m}}^{n+1,k+1}-\tilde{C}_{i,\mathrm{m}}^{n+1,k+1}}{\triangle t}+\zeta\left(C_{i,\mathrm{m}}^{n+1,k+1}-C_{i,\mathrm{im}}^{n+1,k+1}\right)=0, \\
\varphi_{\mathrm{im}} R_{\mathrm{im}}\frac{C_{i,\mathrm{im}}^{n+1,k+1}-C_{i,\mathrm{im}}^{n}}{\triangle t}+\lambda\varphi_{\mathrm{im}} R_{\mathrm{im}} C_{i,\mathrm{im}}^{n+1,k+1}=\zeta\left(C_{i,\mathrm{m}}^{n+1,k+1}-C_{i,\mathrm{im}}^{n+1,k+1}\right).
\end{cases}$$

The first substep of this scheme explicitly calculates the problem of convective transport taking into account the sources and sinks in the right-hand side. Note that in the case of a source, $C_{i,\mathrm{m}}^{n+1}$ is the contaminant concentration in the source averaged over time step, and in the case of a drain $C_{i,\mathrm{m}}^{n+1}$ is approximated explicitly, that is, $C_{i,\mathrm{m}}^{n+1}=C_{i,\mathrm{m}}^{n}$. On the second substep, the problem of diffusion and radioactive decay is implicitly calculated. On the third substep, again, the problem of mass exchange between the flow and non-current zones is implicitly solved. In case of implicit approximation of the convection problem, substeps I and II are aggregated, and the intermediate concentration $\hat{C}_{i,\mathrm{m}}^{n+1,k+1}$ is eliminated.

We now explain the verification of the convergence criterion for a nonlinear solver. As the criterion of convergence it is proposed to use the following expression. The user initially sets two values: $\varepsilon_{\mathrm{rel}}, \varepsilon_{\mathrm{abs}}$. It is assumed that the convergence is achieved when one of two conditions is satisfied:

$$\max\left(\left\|h^{n+1,k}\right\|,\left\|h^{n+1,k+1}\right\|\right)<\varepsilon_{\mathrm{abs}} \tag{19}$$

or

$$\frac{\left\|h^{n+1,k} - h^{n+1,k+1}\right\|}{\max\left(\left\|h^{n+1,k}\right\|, \left\|h^{n+1,k+1}\right\|\right)} < \varepsilon_{\text{rel}}. \tag{20}$$

The checking of the condition (19) being fulfilled before the condition (20) ensures that the error of division by zero does not occur.

4 Parallel Solution of the Models

We have performed the numerical solution of several models with the GeRa computational code. The INM RAS cluster [15] was used. The configuration of the cluster is the following:

- x6core: Compute Node Asus RS704D-E6, 12 nodes (two 6-node processor Intel Xeon X5650@2.67 GHz), 24 GB RAM;
- x8core: Compute Node Arbyte Alkazar+ R2Q50, 16 nodes (two 8-node processor Intel Xeon E5-2665@2.40 GHz), 64 GB RAM;
- x10core: Compute Node Arbyte Alkazar+ R2Q50, 20 nodes (two 10-node processor Intel Xeon E5-2670v2@2.50), 64 GB RAM;
- x12core: Compute Node Arbyte Alkazar+ R2Q50, 4 nodes (two 12-node processor IntelXeon E5-2670v3@2.30 GHz), 64 GB RAM.

The last 3 types of nodes x8core, x10core, and x12core can be used together as a single queue "e5core".

For the solution of linear systems we have exploited the package PETSc. The BiCGstab iterations were performed for Additive Schwarz preconditioning with overlap size 1 and ILU(k=1) as a subdomain solver. The relative tolerance stopping criterion 10^{-9} was applied.

4.1 Model "Lake"

As a sample test we have used the simple model "Lake". The model domain has an impermeable boundary and contains a lake with dense brine. A production well is working forcing the upper cells in the model to unsaturated conditions and the dense brine from the lake to move in the well direction and sink down as well.

The timestep was 10 days, while the total number of timesteps was 37. The total number of cells in a small size model ("Lake-small") was 37100 and the one in a medium size model ("Lake-medium") was 263020.

The computations were performed in the queue "x6core". In all tables below we have used the following notation: "#proc" denotes the number of cores used; "Time" is the total solution time; "Speedup" is the actual speedup with respect to the run on 1 core; S_2 is the relative speedup with respect to the previous run on the 2 times less number of cores.

In Tables 1 and 2 the numerical results for Lake-small and Lake-medium models are presented. The results show quite reasonable speedup, it was equal to 11.92 for 32 cores for a small size model and 41.15 for 128 cores for a medium size model.

Table 1. Lake-small model.

#proc	Time	Speedup	S_2
1	662.99	1.00	—
2	391.35	1.69	1.69
4	216.62	3.06	1.80
8	118.28	5.60	1.83
16	71.76	9.23	1.64
32	55.59	11.92	1.29

Table 2. Lake-medium model.

#proc	Time	Speedup	S_2
1	7118.78	1.00	—
2	4203.46	1.69	1.69
4	2427.53	2.93	1.73
8	1508.87	4.71	1.60
16	901.24	7.89	1.67
32	423.53	16.80	2.12
64	243.23	29.26	1.74
128	172.97	41.15	1.40

4.2 Model “Polygon”

For a real process modelling we have used the model “Polygon”, which is actually a model of the “Severny” LRW injection site. The model contains ten geological layers. LRW is injected in the 9-th and the 5-th layers (aquifer I and aquifer II respectively). Dense brines are injected in layer 9, while in the 5-th layer the density varies only several grams per liter. In this test we show the first application of the new numerical model to the real site and assess its parallel efficiency.

The total number of cells in a small size model (“Polygon-small”) was 43524 and the one in a large size model (“Polygon-large”) was 421033. Figures 1 and 2 demonstrate the mesh distribution over 64 processors for Polygon-large model. One can see the geological fault line as well as regions with mesh refinement over numerous wells. Figure 3 shows the computational results with contaminant concentration distribution for the Polygon-large model.

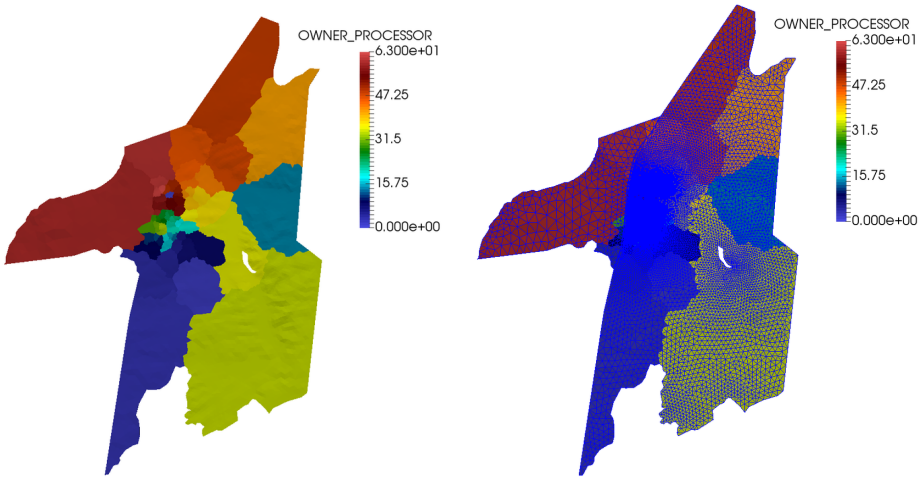

Fig. 1. Distribution of the mesh over 64 processors for Polygon-large model.

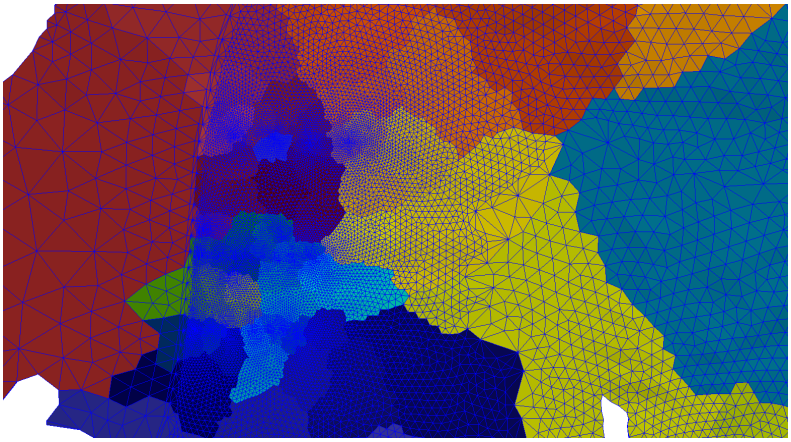

Fig. 2. Fragment of mesh distribution over 64 processors for Polygon-large model.

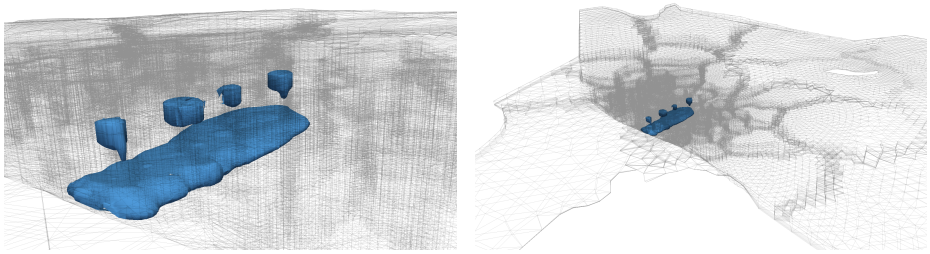

Fig. 3. The contaminant plume position forecast calculated using Polygon-large model.

The timestep in both cases was 10 days, while the total number of timesteps was 183 and 1608, for small and large size models, respectively. The computations were performed in x6core and e5core queues for the above two models, respectively.

In Tables 3 and 4 the numerical results for Polygon-small and Polygon-large models are presented. Results show reasonable speedup for such a complicated problem, it was equal to 13.32 for 32 cores for a small size model and 31.54 for 256 cores for a large size model. Thus we show program scalability for a moderate number of processors. Transition to massively parallel computations is a next task in GeRa development, which is dominated by the parallel efficiency of the solvers for linear systems arising from implicit flow and diffusion problems discretizations.

Table 3. Polygon-small model.

#proc	Time	Speedup	S_2
1	1104.08	1.00	—
2	642.87	1.71	1.71
4	384.39	2.87	1.67
8	218.83	5.04	1.75
16	142.13	7.76	1.53
32	82.84	13.32	1.71

Table 4. Polygon-large model.

#proc	Time	Speedup	S_2
1	67214.51	1.00	—
2	45161.05	1.48	1.48
3	22870.51	2.93	1.97
8	18147.68	3.70	1.26
16	9470.35	7.09	1.91
32	7515.65	8.94	1.26
64	5013.85	13.40	1.49
128	3150.89	21.33	1.59
256	2130.66	31.54	1.47

5 Conclusion

A mathematical model of flow and transport in geological media is proposed, which takes into account the flow in unconfined conditions, dual porosity and variable density of solutions. Based on the analysis of processes applied to the disposal of LRW "Severny", simplifications of the model are proposed. The model is numerically implemented in the GeRa code and tested with respect to the LRW injection polygon. The results of parallel runs show a good scalability of computations up to 256 computational cores. The novel model will be used further for the assessment of the role of density effects on the deep well radioactive waste injection sites.

References

1. Rybalchenko A.I., Pimenov M.K., Kostin P.P., et al.: Deep disposal of liquid radioactive waste, IzdAT, Moscow, 256 p. (1994) (in Russian)
2. Compton K.L., Novikov V., Parker F.L.: Deep Well Injection of Liquid Radioactive Waste at Krasnoyarsk-26, Vol. I, RR-00-1, Int. Inst. for Applied Systems Analysis, Laxenburg, Austria (2000)
3. Kapyrin I.V., Ivanov V.A., Kopytov G.V., Utkin S.S.: Integral code GeRa for the safety substantiation of disposal of radioactive waste. Mountain J., No. 10, pp. 44–50 (2015) (in Russian)
4. Kapyrin I.V., Konshin I.N., Kopytov G.V., Nikitin K.D., Vassilevski Yu.V.: Hydrogeological modeling in problems of safety substantiation of radioactive waste burials using the GeRa code. Supercomputer Days in Russia: Proc. of the Int. Conf. (September 28–29, 2015, Moscow). Publishing House of Moscow State University, Moscow, pp. 122–132 (2015) (in Russian)
5. Plenkin A.V., Chernyshenko A.Yu., Chugunov V.N., Kapyrin I.V.: Methods of constructing adaptive unstructured grids for solving hydrogeological problems. Computational Methods and Programming, Vol. 16, pp. 518–533 (2015) (in Russian)
6. Hammond G. E., Lichtner P. C., Mills R. T. Evaluating the performance of parallel subsurface simulators: An illustrative example with PFLOTRAN. Water resources research. Vol.50, No.1, Pp. 208-228 (2014).

7. Freedman V. L. et al. A high-performance workflow system for subsurface simulation. Environmental Modelling & Software, Vol. 55, 176-189 (2014).
8. Zhang K., Wu Y. S., Pruess, K. User's guide for TOUGH2-MP-A massively parallel version of the TOUGH2 code (No. LBNL-315E). Ernest Orlando Lawrence Berkeley National Laboratory, Berkeley, CA (US), (2008).
9. Lekhov A.V.: Physical-chemical hydrogeodynamics, KDU, 2010, 500 p. (2010) (in Russian)
10. Rabinovich V.A., Khavin Z.Ya.: Brief chemical reference book, Leningrad, 392 p. (1978) (in Russian)
11. Simunek J., Van Genuchten M.T., Sejna M.: The HYDRUS-1D software package for simulating the movement of water, heat, and multiple solutes in variably saturated media, version 3.0, HYDRUS software series 1. Department of Environmental Sciences, Univ. of California Riverside (2005)
12. Diersch H.J.: FEFLOW-white papers, vol. I. WASY GmbH Inst. for water resources planning and systems research, Berlin, 366 p. (2005)
13. Liu X.: Parallel modeling of three-dimensional variably saturated ground water flows with unstructured mesh using open source finite volume platform OpenFOAM. Engineering Applications of Computational Fluid Mechanics, Vol. 7, No. 2, pp. 223–238 (2013)
14. Paniconi C., Putti M.: A comparison of Picard and Newton iteration in the numerical solution of multidimensional variably saturated flow problems. Water Resources Research, Vol. 30, No. 12, pp. 3357–3374 (1994)
15. INM RAS cluster. URL: http://cluster2.inm.ras.ru (accessed: 15.04.2018) (in Russian)